Ordered Nanowire Array Blue/Near-UV Light Emitting Diodes

By *Sheng Xu, Chen Xu, Ying Liu, Youfan Hu, Rusen Yang, Qing Yang, Jae-Hyun Ryou, Hee Jin Kim, Zachary Lochner, Suk Choi, Russell Dupuis,* and *Zhong Lin Wang**

ZnO-based light emitting diodes (LEDs) have been considered as a potential candidate for the next generation of blue/near-UV light sources,[1] due to a direct wide bandgap energy of 3.37 eV, a large exciton binding energy of 60 meV at room temperature, and several other manufacturing advantages of ZnO.[2] While the pursuit of stable and reproducible p-ZnO is still undergoing,[3,4] heterojunctions of n-ZnO and p-GaN are employed as an alternative approach in this regard by considering the similar crystallographic and electronic properties of ZnO and GaN.[5–7] Compared with the thin film/thin film LEDs,[5,6,8] which may suffer from the total internal reflection, n-ZnO nanowire/p-GaN thin film heterostructures are utilized in order to increase the extraction efficiency of the LEDs by virtue of the waveguiding properties of the nanowires.[9–11] But in all of these cases, the n-ZnO nanowires are randomly distributed on the substrate, which largely limits their applications in high performance optoelectronic devices.

Here in this work, we demonstrate the capability of controlling the spatial distribution of the blue/near-UV LEDs composed of position controlled arrays of n-ZnO nanowires on a p-GaN thin film substrate. The device was fabricated by a conjunction of low temperature wet chemical methods and electron beam lithography (EBL). The EBL could be replaced by other more convenient patterning techniques, such as photolithography and nanosphere lithography, rendering our technique low cost and capable of scaling up easily. Under forward bias, each single nanowire is a light emitter. By Gaussian deconvolution of the emission spectrum, the origins of the blue/near-UV emission are assigned particularly to three distinct electron-hole recombination processes. By virtue of the nanowire/thin film heterostructures, these LEDs give an external quantum efficiency of 2.5%. This approach has great potential applications in high resolution electronic display, optical interconnect, and high density data storage.

The design of the LED is shown in **Figure 1a**. Ordered ZnO nanowire arrays were grown on p-GaN (Figure 1b–d),[12–14] The capability of controlling the positions of the nanowires on the substrate allows us to fabricate nanoscale light emitters in a controllable pattern.[15] Ohmic contacts to the bottom p-GaN and top n-ZnO nanowires were made, as confirmed by their individual *I–V* curves (Supporting Information (SI) Figure S1 inset), and the rectifying *I–V* curve (Figure S1) comes only from the p-n diode herein. Figure 1e is the optical image of a lighted up LED at a biased voltage of 10 V. In the device, all of the nanowires are connected in parallel and each single nanowire is a light emitter. Brightness difference among the individual nanowires comes probably from the current crowding effect and different serial contact resistances therefore different injection currents through the individual nanowire. The pitch between each lighting spot shown in Figure 1e is 4 µm and the resolution is 6350 dpi.

The physical origin of this electroluminescence (EL) has been extensively studied but is still under debate.[16,17] As shown in **Figure 2a**, emission spectrum of the as-fabricated LED was monitored at different biased voltages/injection-currents at room temperature. We can see that, from 4 V to 10 V, the contour of the EL spectrum does not change much with the biased voltage. The dominant emission peak is slightly blue shifted in the range of 400 nm–420 nm with a full width at half maximum (FWHM) of about 60 nm. The peak intensity versus injection current (L–I^m) characteristics have been acquired (Figure S2), showing a superlinear relationship with $m = 1.3$. Peak-deconvolution with Gaussian functions, inset picture in Figure 2a, shows that the broad spectrum consists of three distinct bands (Figure 2b) centered in the range of 395–415 nm, 420–440 nm, and 450–510 nm, respectively, and each emission band corresponds to a particular recombination process as elaborated in the following. The near-UV emission band centered at around 400 nm is attributed to the near band edge (NBE) emission in ZnO nanowires that originates from the recombination of ZnO free and bound excitons.[18,19] Whereas the red shifted violet emission band centered at about 430 nm is ascribed to the transitions from the conduction band or shallow donors to deep Mg acceptor levels in the p-GaN thin film substrate.[5,18,19] The blue emission around 460 nm comes from the radiative interfacial recombination of the electrons from n-ZnO and holes from p-GaN.[18,20,21]

There has been a controversy about whether the emission is from the n-ZnO side[15,22] or the p-GaN side.[5,19] Here, from our observation, both scenarios have made contributions. In reality, the hole concentration in the Mg-doped p-GaN substrate (p ~ 10^{18} cm^{-3}) is higher than the electron concentration in the n-ZnO nanowire (n ~ 10^{17} cm^{-3}), but the carrier mobility in the p-GaN is smaller than that in the n-ZnO. The barrier heights at

[*] S. Xu, C. Xu, Y. Liu, Y. F. Hu, R. S. Yang, Q. Yang, Prof. Z. L. Wang
School of Materials Science and Engineering
Georgia Institute of Technology
Atlanta, Georgia, 30332–0245 (USA)
E-mail: zlwang@gatech.edu
J. H. Ryou, H. J. Kim, Z. Lochner, S. Choi, Prof. R. Dupuis
School of Electrical and Computer Engineering
Georgia Institute of Technology
Atlanta, Georgia, 30332–0245 (USA)

DOI: 10.1002/adma.201002134

© 2010 WILEY-VCH Verlag GmbH & Co. KGaA, Weinheim

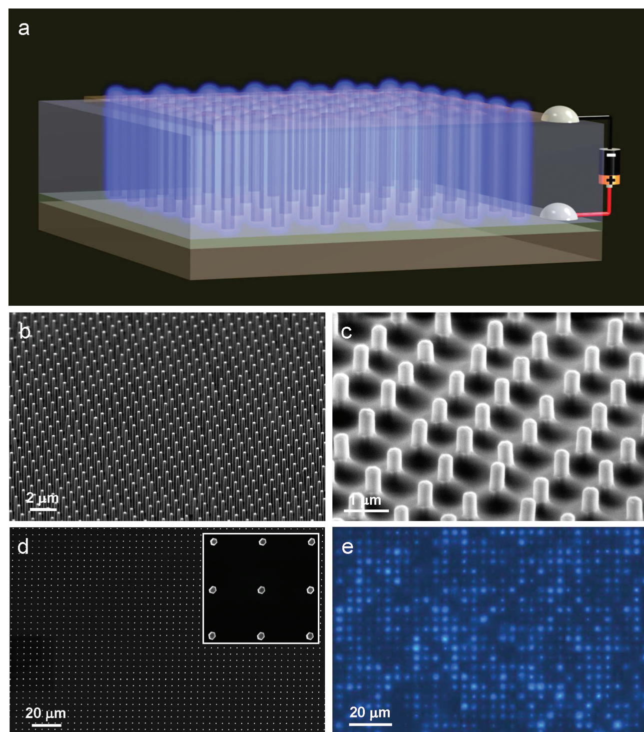

Figure 1. (a) Design overview of the LED. (b) 60° tilt SEM view of the as-grown patterned vertical ZnO nanowires with a width about 300 nm and (c) after they are coated with SiO_2 and wrapped with PMMA, and the tips are exposed. (d) Top SEM image of the ZnO nanowire arrays. The pitch and layout of the nanowire arrays are readily controlled by the EBL. (e) The optical image of a turned on LED (artificial bluish color).

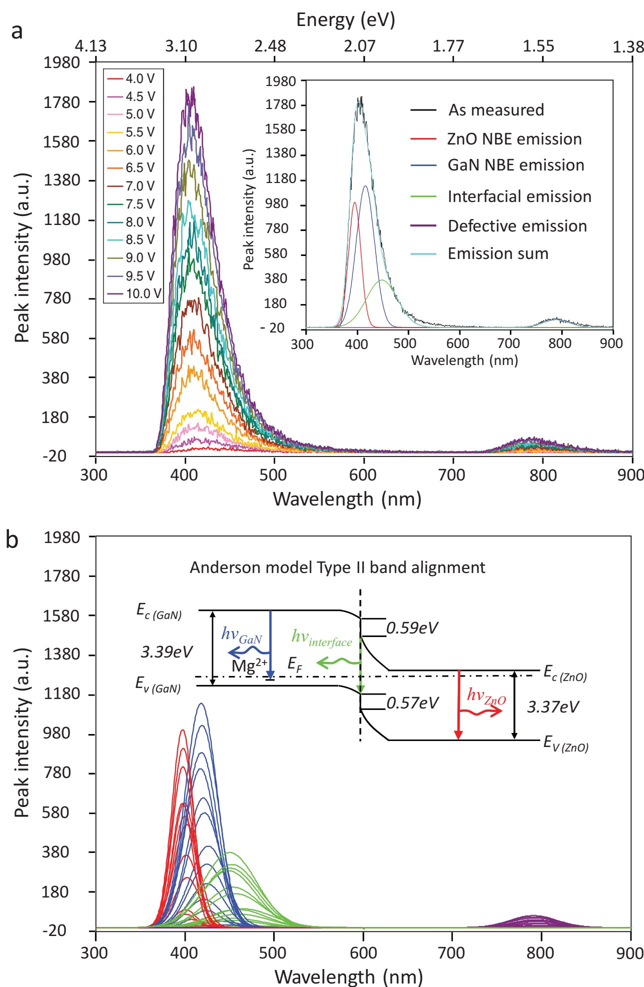

Figure 2. (a) EL spectrum as a function of the forward biased voltage. Inset shows by Gaussian deconvolution analysis the blue/near-UV emission could be decomposed into three distinct bands that correspond to three different optoelectronic processes. (b) All of the four emission bands evolve (band width, height, and intensity) as a function of the biased voltage. Inset schematics show the band diagram of the n-ZnO/p-GaN heterojunction under no or small biased voltage, where the three emission bands comprising the blue/near UV light are specifically indicated in different colors.

the interface for the holes (0.57 eV) and for the electrons (0.59 eV) are comparably equal. In that case, the charge injection by electrons and holes should be comparable from both sides. Of course, the energy band offset at the ZnO/GaN interface is likely to be determined by the fabrication process.[23] The blue emission around 460 nm is related to the radiative interfacial recombination of the electrons from n-ZnO and holes from p-GaN.[18,20,21] The interface states generally act as nonradiative centers that annihilate free electrons and holes. Therefore, it is required to get high quality interface between the heterojunctions in order to get high efficiency LEDs. The weak red emission at around 790 nm is coming from the native deep level point defects (oxygen vacancies and zinc interstitials) in ZnO nanowires.[19]

As the biased voltage is increased, intensity of the main peak and all of the four sub-bands (including the defect emission) exponentially increases and also blue shifts (Figure 2b and Figure S3 in SI). The blue shift has been explained to be caused by several different mechanisms, such as band renormalization and band filling,[24] and the screening effect of the built-in piezoelectric field.[25] Here in our experiment, the blue shift of the emission peak comes from two resources: the blue shift of sub-band positions (**Figure 3a**), and the change of relative intensities of the sub-bands at different injection currents (Figure 3b).[18] The blue shift of the ZnO and GaN NBE emission positions (Figure 3a i and ii) may be caused by the recombination of increasing kinetic energies of electrons and holes as the biased voltage is increased (assuming the mobility of the carriers does not change too much when the biased voltage is not too high), and that could contribute to the energy of the emitted photons. The most obvious blue shift of the peak position comes from the interfacial recombination process (Figure 3a iii), which is simply because the kinetic energy increases from both electrons and holes contribute to the interfacial recombination.

The blue shift of the EL spectrum also comes from the change of the relative intensity of the three bands, as shown in Figure 3b (see Figure S4 in SI for the peak heights and peak widths, respectively). The intensity of the GaN NBE emission increases comparatively faster than the ZnO NBE emission and

© 2010 WILEY-VCH Verlag GmbH & Co. KGaA, Weinheim

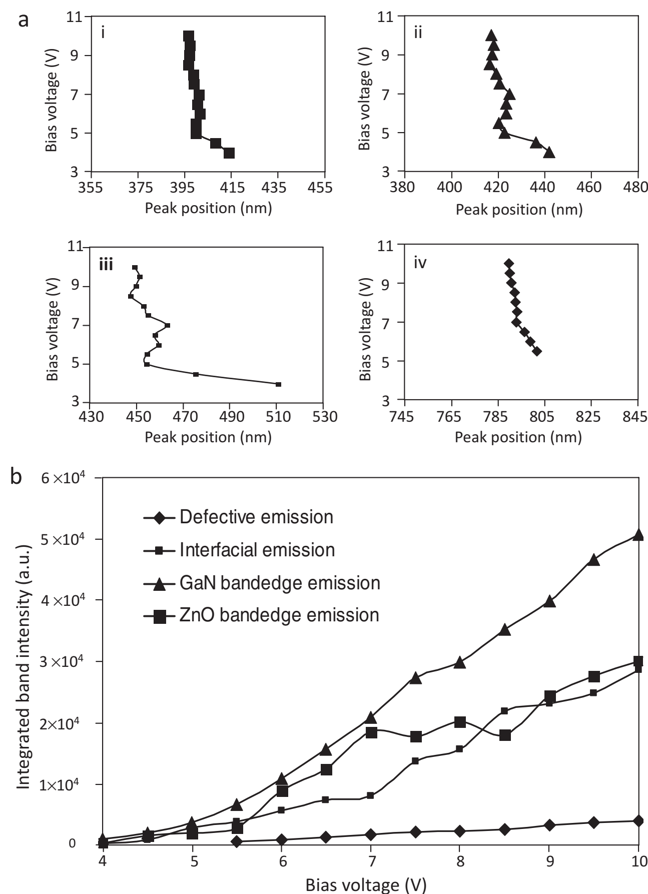

Figure 3. (a) Peak positions blue shift as a function of the biased voltage for (i) ZnO NBE emission, (ii) GaN NBE emission, (iii) interfacial emission, and (iv) defective emission. (b) The integrated emission bands intensity as a function of the biased voltage. For the defective emission, when the biased voltage is below 5.5 V, it is hardly distinguished from the noise level.

the interfacial emission. As the biased voltage is increased, the band bending of the p-GaN and n-ZnO is reduced, therefore the kinetic energy of the electrons and holes is increased and they have much higher probability to go across the interface barrier and recombine at the other side. As we compare the curve for ZnO NBE and the one for GaN NBE emissions (Figure 3b), at low biased voltages (<7.0 V), the ZnO NBE emission has a competitive intensity with the GaN counterpart. As the biased voltage goes up, the ZnO NBE emission falls behind the GaN. In comparison with the high quality GaN thin film fabricated by MOCVD, the relatively high level of native defects with the hydrothermally grown ZnO nanowires could undermine its internal quantum efficiency, especially when the biased voltage is relatively high. These point defects in the ZnO nanowires perform like trapping centers and give rise to nonradiative recombinations.

As the flat thin film based LEDs are suffering from the low light extraction efficiency as limited by the total internal reflection, extensive research efforts have been made in this regard, such as roughing the surface of the emitting thin film,[26] reshaping the geometry of the LED architechture,[27] utilizing resonant cavity,[28] coupling with surface plasmon,[29] and fabricating photonic crystal structures,[30] etc. Among these approaches, nanowire/thin film heterostructures are proposed to be a promising method considering the feasible waveguiding properties of ZnO nanowires.[9–11,31–33] Under the single mode waveguide cavity conditions, $V = 2\pi \frac{a}{\lambda_o}\left(n_1^2 - n_2^2\right)^{\frac{1}{2}} = 2.405$,[11] 86.5% of the light would be confined within a 223 nm nanowire, where V is the single mode cut-off value, a is the diameter of the nanowire, λ_o is the free space wavelength of the propagating light (here we set it to be 400 nm), and n_1(2.10) and n_2 (1.59) are the effective refractive index of the ZnO nanowire and the cladding PMMA thin film, respectively. To note, the facets of the nanowire are assumed to be perfectly flat under the single mode conditions. But in reality, these nanowires have rounded tips (Figure 2b), a large surface to volume ratio, and thus a high density of surface states near the band edge, which allows a great reduction of the back reflections at the ZnO nanowire surfaces, known as the omnidirectional reflector effect.[34] Besides, based on an effective medium theory, these graded refractive indices of GaN (2.49), ZnO (2.10), PMMA (1.59) and air (1.0) could largely reduce the Fresnel reflection between GaN/ZnO, ZnO/PMMA, and PMMA/air interfaces, which helps the optical transmission. By virtue of these advantages, the light could easily be extracted out through multiple scattering. ZnO have a transmittance of over 90% in the visible range,[10] so the self-absorption of the nanowires should not be the major concern. To take one step further, the patterned ZnO nanowire arrays form a two-dimensional photonic crystal, which has an optical bandgap for the light travelling parallel to the surface of the substrate. So by controlling the periodicity of the nanowire arrays, it may be possible to match the wavelength of the emitted light to the bandgap of the photonic crystal, possibly resulting in normal directional emission of the light.

Figure 4 shows the room temperature external quantum efficiency versus d.c. injection current characteristics. The external quantum efficiency was calculated by acquiring the ratio of the

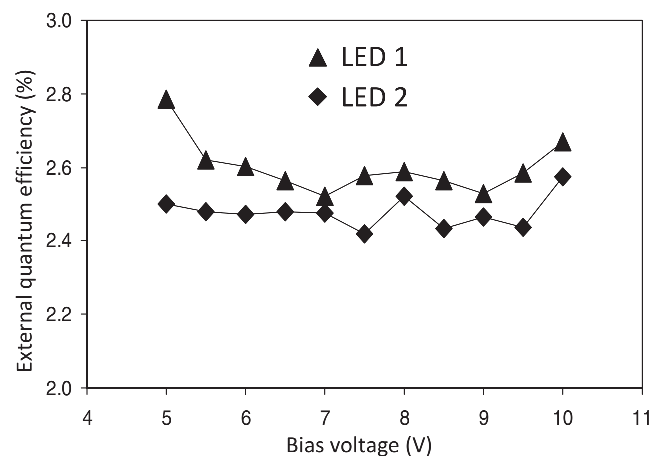

Figure 4. External quantum efficiencies of two heterostructural LEDs as a function of the biased voltage/injection current. The efficiency was determined only when the LED was turned on and the light output power was stably registered with the power meter.

© 2010 WILEY-VCH Verlag GmbH & Co. KGaA, Weinheim

output light power and the input electrical power (Table S1 in SI). As we clearly see, the external quantum efficiency of the LED is about 2.5%, which is considerably high for a single p-n junction based LEDs, and such data are reproducible and consistent for several devices. As the biased voltage/injection current is gradually increased, the external quantum efficiency becomes steady, which indicates that the serial resistance or the nonradiative recombination through the defects, e.g. Auger recombination, does not increase in proportion with increasing the injection current.

In summary, we demonstrated the capability of controlling the spatial distribution of the blue/near-UV light emitting diodes, utilizing ordered arrays of n-ZnO nanowires on a p-GaN thin film substrate by a conjunction of EBL and low temperature wet chemical methods. Under forward bias, each single nanowire is a light emitting emitter. By Gaussian deconvolution analysis of the emission spectrum, the origins of the blue/near-UV emission are assigned to three distinct electron-hole recombination processes. By virtue of these nanowire/thin film heterostructures, these LEDs give an external quantum efficiency of 2.5%. This study has great potential applications in many areas, including solid state lighting, high resolution electronic panel display, optical interconnect, and high density information storage.

Experimental Section

Fabrication of the LEDs: After the growth of ZnO nanowire arrays, a 30-nm by 30-nm layers of Ni/Au were deposited by electron beam evaporation on the p-GaN followed by rapid thermal annealing in air at 500 °C for 5 min. A 50-nm conformal layer of SiO_2 was deposited onto the nanowire arrays by PECVD. After that, a relatively thick layer of PMMA (MICROCHEM) was carefully spun coated onto the substrate to wrap around the nanowires. During this process, the SiO_2 layer protected the nanowires from falling down onto the substrate due to the surface tension of the PMMA. Then oxygen plasma was applied to etch away the top part of the PMMA followed by RIE to remove the top SiO_2, exposing the tips of the nanowires. Since the oxygen plasma and RIE were only applied to the tip part of the nanowires, the damage/deterioration they might have induced to the electrical and optical properties of the nanowires could be neglected. Then, a 100-nm layer of ITO was sputtered as the top common electrode of nanowires.

Characterization of the LEDs: The morphology of the ZnO nanowire arrays was characterized by LEO 1550 SEM. The forward biased voltage was applied by Semiconductor Characterization System Keithley 4200. The optical image of the blue/near-UV light was recorded under Nikon Eclipse Ti inverted fluorescence microscope with 9 s exposure time and a gain value of 1. The EL spectrum was measured on a Master Systems Felix32 PTI fluorescence detector. When measuring the EL spectrum, the device was let cool down before doing another measurement so the possible thermal effect could be ignored. The fitting of the EL spectrum was performed using the Microcal Origin software. The external quantum efficiency of the LEDs was measured using a power meter (OPHIR, NOVA-ORIEL, P/N 1Z01502) and a light detector (OPHIR, 3A-P-SH-V1, P/N 1Z02622).

Supporting Information

Supporting Information is available from the Wiley Online Library or from the author.

Acknowledgements

Research supported by NSF (DMS 0706436, CMMI 0403671, ENG/CMMI 112024), BES DOE (DE-FG02–07ER46394).

Received: June 10, 2010
Revised: July 3, 2010
Published online:

[1] A. Tsukazaki, A. Ohtomo, T. Onuma, M. Ohtani, T. Makino, M. Sumiya, K. Ohtani, S. F. Chichibu, S. Fuke, Y. Segawa, H. Ohno, H. Koinuma, M. Kawasaki, *Nat. Mater.* **2005**, *4*, 42.
[2] Y. I. Alivov, E. V. Kalinina, A. E. Cherenkov, D. C. Look, B. M. Ataev, A. K. Omaev, M. V. Chukichev, D. M. Bagnall, *Appl. Phys. Lett.* **2003**, *83*, 4719.
[3] D. C. Look, B. Claflin, Y. I. Alivov, S. J. Park, *Phys. Status Solidi a-Appl. Res.* **2004**, *201*, 2203.
[4] B. Xiang, P. W. Wang, X. Z. Zhang, S. A. Dayeh, D. P. R. Aplin, C. Soci, D. P. Yu, D. L. Wang, *Nano Lett.* **2007**, *7*, 323.
[5] Y. I. Alivov, J. E. Van Nostrand, D. C. Look, M. V. Chukichev, B. M. Ataev, *Appl. Phys. Lett.* **2003**, *83*, 2943.
[6] R. D. Vispute, V. Talyansky, S. Choopun, R. P. Sharma, T. Venkatesan, M. He, X. Tang, J. B. Halpern, M. G. Spencer, Y. X. Li, L. G. Salamanca-Riba, A. A. Iliadis, K. A. Jones, *Appl. Phys. Lett.* **1998**, *73*, 348.
[7] T. P. Yang, H. C. Zhu, J. M. Bian, J. C. Sun, X. Dong, B. L. Zhang, H. W. Liang, X. P. Li, Y. G. Cui, G. T. Du, *Mater. Res. Bull* **2008**, *43*, 3614.
[8] H. Asil, E. Gur, K. Cinar, C. Coskun, *Appl. Phys. Lett.* **2009**, *94*, 253501.
[9] J. Zhong, H. Chen, G. Saraf, Y. Lu, C. K. Choi, J. J. Song, D. M. Mackie, H. Shen, *Appl. Phys. Lett.* **2007**, *90*, 203515.
[10] S. J. An, J. H. Chae, G. C. Yi, G. H. Park, *Appl. Phys. Lett.* **2008**, *92*, 121108.
[11] K. S. Kim, S.-M. Kim, H. Jeong, M. S. Jeong, G. Y. Jung, *Adv. Funct. Mater.* **2010**, *20*, 1076.
[12] S. Xu, Y. Wei, M. Kirkham, J. Liu, W. Mai, D. Davidovic, R. L. Snyder, Z. L. Wang, *J. Am. Chem. Soc.* **2008**, *130*, 14958.
[13] S. Xu, C. Lao, B. Weintraub, Z. L. Wang, *J. Mater. Res.* **2008**, *23*, 2072.
[14] S. H. Park, S. W. Han, *J. Nanosci. Nanotechnol.* **2007**, *7*, 2526.
[15] J. J. Cole, X. Wang, R. J. Knuesel, H. O. Jacobs, *Nano Lett.* **2008**, *8*, 1477.
[16] K. A. Bulashevich, I. Y. Evstratov, S. Y. Karpov, *Phys. Status Solidi a-Appl. Mater. Sci.* **2007**, *204*, 241.
[17] I. E. Titkov, A. S. Zubrilov, L. A. Delimova, D. V. Mashovets, I. A. Liniichuk, I. V. Grekhov, *Semiconductors* **2007**, *41*, 564.
[18] A. M. C. Ng, Y. Y. Xi, Y. F. Hsu, A. B. Djurisic, W. K. Chan, S. Gwo, H. L. Tam, K. W. Cheah, P. W. K. Fong, H. F. Lui, C. Surya, *Nanotechnology* **2009**, *20*, 445201.
[19] H. Y. Xu, Y. C. Liu, Y. X. Liu, C. S. Xu, C. L. Shao, R. Mu, *Appl. Phys. B-Lasers Opt.* **2005**, *80*, 871.
[22] R. Guo, J. Nishimura, M. Matsumoto, M. Higashihata, D. Nakamura, T. Okada, *Appl. Phys. B-Lasers Opt* **2009**, *94*, 33.
[23] H. F. Liu, G. X. Hu, H. Gong, K. Y. Zang, S. J. Chua, *J. Vac. Sci. Technol. A* **2008**, *26*, 1462.
[20] Y. I. Alivov, U. Ozgur, S. Dogan, C. Liu, Y. Moon, X. Gu, V. Avrutin, Y. Fu, H. Morkoc, *Solid State Electron.* **2005**, *49*, 1693.
[21] X. M. Zhang, M. Y. Lu, Y. Zhang, L. J. Chen, Z. L. Wang, *Adv. Mater.* **2009**, *21*, 2767.
[24] C. Bayram, F. H. Teherani, D. J. Rogers, M. Razeghi, *Appl. Phys. Lett.* **2008**, *93*, 081111.

© 2010 WILEY-VCH Verlag GmbH & Co. KGaA, Weinheim

[25] H. W. Choi, C. W. Jeon, M. D. Dawson, P. R. Edwards, R. W. Martin, S. Tripathy, *J. Appl. Phys.* **2003**, *93*, 5978.
[26] I. Schnitzer, E. Yablonovitch, C. Caneau, T. J. Gmitter, A. Scherer, *Appl. Phys. Lett.* **1993**, *63*, 2174.
[27] H. Kim, K.-K. Kim, K.-K. Choi, H. Kim, J.-O. Song, J. Cho, K. H. Baik, C. Sone, Y. Park, T.-Y. Seong, *Appl. Phys. Lett.* **2007**, *91*, 023510.
[28] E. F. Schubert, J. K. Kim, *Science* **2005**, *308*, 1274.
[29] W. L. Barnes, *J. Lightwave Technol.* **1999**, *17*, 2170.
[30] T. N. Oder, K. H. Kim, J. Y. Lin, H. X. Jiang, *Appl. Phys. Lett.* **2004**, *84*, 466.
[31] K. K. Kim, S. D. Lee, H. Kim, J. C. Park, S. N. Lee, Y. Park, S. J. Park, S. W. Kim, *Appl. Phys. Lett.* **2009**, *94*, 071118.
[32] E. Lai, W. Kim, P. D. Yang, *Nano Res.* **2008**, *1*, 123.
[33] H. Sekiguchi, K. Kato, J. Tanaka, A. Kikuchi, K. Kishino, *Phys. Stat. Sol.* **2008**, *205*, 1067.
[34] S. H. Park, S. H. Kim, S. W. Han, *Nanotechnology* **2007**, *18*, 055608.

© 2010 WILEY-VCH Verlag GmbH & Co. KGaA, Weinheim